Diffusion and Dimer Formation of CO Molecules Induced by Femtosecond Laser Pulses

Michael Mehlhorn, Heiko Gawronski, and Karina Morgenstern

Abteilung ATMOS, Leibniz Universität Hannover, Appelstrasse 2, 30167 Hannover, Germany

(Received 23 September 2009; published 19 February 2010)

We investigate two fundamental steps of a nonadiabatic surface process, the photo-induced movement and approach of CO molecules on the Cu(111) surface, at a hitherto unachieved single-molecule level through scanning tunneling microscope imaging. For the close approach of two CO molecules, we not only determine the nonadiabatic diffusion barrier (87 meV), but also discover a femto-second-laser-induced transient attraction (30 meV) of the usually repelling CO molecules.

DOI: 10.1103/PhysRevLett.104.076101 PACS numbers: 68.37.Ef, 82.37.Gk, 82.53.St

The understanding and selective control of elementary steps of surface reactions is an important goal in surface science. From the experimental point of view, the use of photons as the energy source facilitates identification of the elementary steps by varying, e.g., polarity, energy, or fluence. For photon-induced surface processes, one must distinguish between three different excitation mechanisms. The first possibility is resonant photon absorption through the adsorbate. The second excitation occurs through adiabatic coupling of the molecules to the laser-heated substrate lattice. In the third mechanism, laser-excited substrate electrons (hot electrons) drive the process directly. This last mechanism is distinguished by intense ultra short laser pulses that allow the electronic excitation of the metal substrate and the energy transfer to phonons to be differentiated in time.

In addition, the high density of excited electrons after excitation by femtosecond (fs) laser pulses results in a higher yield than in conventional photochemistry. In most cases, the yield has been investigated by detecting the desorbing species, and the higher yield is conventionally explained by multiple excitations [1]. Only two groups were successful in quantitatively investigating fs-laser-induced diffusion from step edges [2,3]. These studies are applicable to diffusion between nonequivalent adsorption sites, but can not differentiate between single-molecule processes and processes of a molecular ensemble. However, we showed recently that the local structure of the water clusters dictates the diffusion [4]. This microscopic understanding of a fundamental step in surface chemistry is based on single-molecule observation, as provided by scanning tunneling microscopy (STM) [5,6].

In this Letter, we use a combination of STM and fs laser to follow the fs-laser-induced lateral motion of individual CO molecules on Cu(111) and the generation of CO dimers. For diffusion, we find two different electron-mediated processes at different laser fluence. By modeling the high fluence regime, we determined a diffusion barrier of $E_{\mathrm{diff}} = 87$ meV and an attempt frequency of $R_0 = 10^{12.6}$ Hz. With a similar modeling, we determine an unexpected transient attraction energy of $E_{\mathrm{attr}} > 30$ meV for the formation of CO dimers. The latter process has important consequences for nonadiabatic surface processes. Our study thus opens a new field of quantitative single-molecule nonadiabatic surface processes.

The experiments were performed with our custom-built instrument that combines single-molecule spatial resolution of a low temperature STM (LT-STM) working at 5 K in ultrahigh vacuum with the ultrafast surface dynamics driven by fs-laser excitation [6]. CO with coverages of a few percent of a monolayer (ML) is deposited onto the Cu(111) sample held at 17 K. Surface processes are induced by frequency doubled laser pulses of a Ti:sapphire oscillator with a duration of 40 fs at 400 nm (3.1 eV photon energy, repetition rate 10 MHz). Focusing onto $10 \times 25\ \mu\mathrm{m}^2$ leads to absorbed fluences in the range of a few $\mathrm{J/m}^2$. Prior to laser irradiation, the tip is retracted by about 200 nm in perpendicular direction from the sample and by more than 1 μm in parallel direction to the sample perpendicular to the laser plane. This rules out far and near field tip effects during the irradiation. Typically, the sample is exposed to 2.5×10^8 pulses with an absorbed fluence from 1.1 to 5.1 $\mathrm{J/m}^2$ [7].

We start by describing our observation qualitatively. In as-deposited CO ensembles, the shortest distance between two adjacent CO molecules is $\sqrt{3}a$ [Fig. 1(a)] with the lattice constant of the substrate $a = 0.255$ nm. This distance is equivalent to the CO nearest-neighbors distance at saturation coverage of 1/3 ML ($\sqrt{3} \times \sqrt{3}R30°$) [8]. $\sqrt{3}$ dimers are imaged as dark ellipsoids [cf. inset and line scan in Figs. 1(a) and 1(c)]. The irradiation with fs-laser pulses leads to the formation of an additional structure, a protrusion between two depressions [Fig. 1(b)]. This type of image is known from manipulation experiments, in which two CO molecules were forced onto two neighboring substrate atoms by LT-STM [9]. The intensity variation was reproduced theoretically and explained by a tilting of the CO molecule axes away from the surface normal [10,11] [Fig. 1(c)] because of a combination of steric repulsion between the molecules and electrostatic repulsion between their dipole moments. Such an arrangement is not stable at elevated temperature because of the repulsion [12]. Thus, the dimer formation induced by fs-laser irradiation indicates a nonadiabatic process.

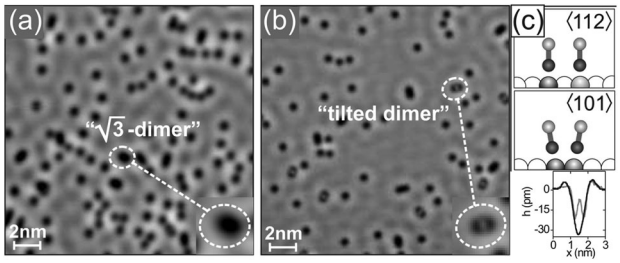

FIG. 1. STM images of CO on Cu(111): (a) 0.05 ML CO deposited at 17 K, CO molecules are imaged as a circular depression [8]; 30 pA, 250 mV, 5 K. (b) 0.03 ML CO after fs-laser excitation with 2×10^9 pulses (400 nm, 40 fs, 3.9–5.1 J/m^2); circle marks tilted dimer; 35 pA, 240 mV, 7 K; insets enlarge different dimer structures. (c) Ball-and-stick model of the $\sqrt{3}$ dimer (top), the tilted dimer (middle), and experimental line scans of $\sqrt{3}$ dimer (black line) and of tilted dimer (light gray line) (bottom).

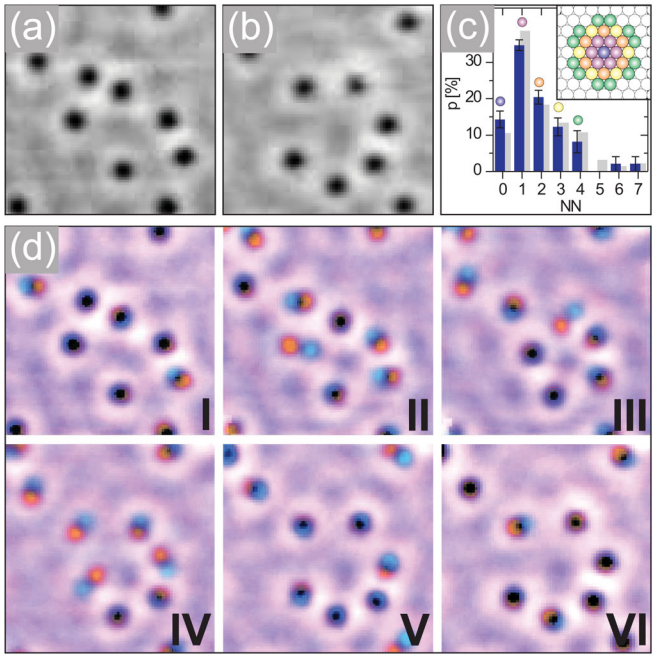

FIG. 2 (color). fs-laser-induced diffusion: (a), (b) STM image before and after excitation series shown in (d) 35 pA, 240 mV, 7 K. (c) Distribution of CO molecules on nearest neighboring (NN) sites based on 1500 hopping events after excitation with 5.1 J/m^2 (dark blue bars) and calculation for random motion (gray bars); error bars represent statistical error; colored ball model indicates equivalent NN adsorption sites on (111) (d) Excitation series: Superposition of STM images taken before and after excitation with 2.5×10^8 pulses for different fluences (I: 1.8 J/m^2, II: 4.9 J/m^2, III: 4.7 J/m^2, IV: 5.1 J/m^2, V: 4.4 J/m^2, and VI: 3.9 J/m^2). Orange (blue) indicates the initial (final) positions of CO molecules that change position, whereas stationary molecules appear black.

Having set the stage, we now turn to the quantitative analysis of the laser-induced processes. First, we determine the diffusion barrier for single noninteracting CO molecules, a result we use below for analysis of the tilted dimer formation. Here, STM allows us to follow the diffusion of individual molecules by repeatedly imaging the same molecules in between irradiation sequences; Figs. 2(a) and 2(b) show the first and last images of such a series. The hopping distribution [Fig. 2(c)] of the CO molecules is determined from image series as shown in Fig. 2(d). The diffusion is then analyzed based on the formalism for thermally induced diffusion by single-hopping events [13]. Instead of the hopping events per time at a constant temperature, we use here the hopping events per pulse at a constant laser fluence (for details, see EPAPS [14]). Because this formalism is only applicable if the diffusion of the molecules is independent from each other, we consider only the diffusion of CO molecules with nearest-neighbors distances larger than 1.5 nm. This analysis excludes long-range interactions mediated by surface-state electrons [15].

For fs-laser-induced processes, the dependence of a yield Y, here the hopping rate per pulse, on absorbed fluence F can be used to determine the underlying energy transfer mechanism and the involved energy barrier [1]. The yield (Fig. 3) increases almost linearly for lower fluence, but at higher fluence, it depends in a strong nonlinear way on F. We rationalize the different regimes based on different energy transfer mechanisms in the case of lower and higher fluence [16–18]. The absorption of a fs-laser pulse results in a high density of photo-excited electrons and holes in the metal. After excitation, the electrons can interact directly with the adsorbed molecule or undergo many-body scattering processes to form a Fermi-like energy distribution, described by an electronic temperature T_{el}, before they interact with the adsorbate (inset of Fig. 3). The thermalization time, i.e., the available time, in which nonthermal electrons interact with the adsorbate, depends on the available phase space for electron-electron scattering and decreases from values around 1 ps for fluences <1 J/m^2 to values <100 fs for 5 J/m^2. Thus, for low fluence, mainly photo-excited electrons interact with the adsorbate, while at higher fluence, thermalized electrons dominate the interaction.

The diffusion driven by photo-excited electrons at low fluences can be explained by the model of dynamics induced by electronic transition (DIET) [1]. In this model, the energy transfer occurs through inelastic scattering of a substrate electron by a negative ion resonance of the adsorbed molecule. Here, the resonance is the orbital deduced from the $2\pi^\star$ orbital of the free CO molecule located at 3.35 eV above the Fermi level with a full-width at half-maximum (FWHM) of 0.6 eV. This state can be reached efficiently by electrons generated from photons with 3.1 eV [19,20]. Anharmonic coupling of the electron-induced internal CO stretch and external CO-Cu bending modes to the frustrated translation and/or rotation facilitates to overcome the energy barrier for diffusion. Such anharmonic coupling was used before to model the STM induced diffusion of CO on Pd [21] and NH_3 on Cu(100) [22] and also fs-laser-induced diffusion of CO on Pt from

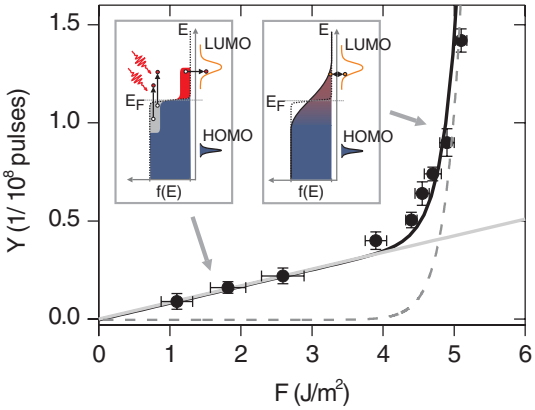

FIG. 3 (color online). Dependence of CO hopping rate per pulse Y on absorbed fluence F (from >10 000 hopping events); modeling of the hopping rate as a sum of a single electron process (dashed line) and EFM with $R_0 = 10^{12.6}$ Hz and $E_d =$ 87 meV (sum in black line); dashed line represents trend of modeling the hopping rate with EFM disregarding photo-excited processes; inset: electron energy distribution before (left) and after (right) thermalization; error bars on yield are statistical error; error bars on fluence result from using data of several experiments with slightly different fluence for better statistics.

step edges [2]. Here, the fluence dependence of the hopping rate is linear (Fig. 3) consistent with one electronic transition per hopping event in DIET.

For diffusion driven mainly by thermalized electrons at higher fluences, we apply the widely used two-temperature model (2TM) [23,24] with the expansion to adsorbate vibrations along the reaction coordinate using a friction formalism (electronic friction model = EFM) [25,26]. The 2TM describes the dynamics of laser-excited electrons and the energy flow between the electronic and the phononic system of the metal substrate. This analysis leads to time-dependent temperatures for the surface temperatures of electrons T_{el} and phonons T_{ph}.

In the EFM [14], the coupling of adsorbate vibrations to the heat bath of the electrons and phonons of the metal sample results in a transient increase of the adsorbate temperature T_{ads}. From T_{ads}, we calculate the hopping rate R_{hop} for each adsorbate temperature: $R_{\mathrm{hop}} = R_0 e^{-E_d/kT_{\mathrm{ads}}}$, where R_0 and E_d denote the attempt frequency and the diffusion energy, respectively. Because the adsorbate temperature changes in time, the hopping rate per pulse is calculated by integrating the hopping rate over the time interval until the initial temperature is recovered: $Y = \int R_{\mathrm{hop}}(t)dt = R_0 \int e^{-E_d/kT_{\mathrm{ads}}(t)}dt$. With this equation, we fit the nonlinear part of the hopping rate in Fig. 3 by varying R_0 and E_d (black line in Fig. 3). We thus determine an attempt frequency of $R_0 = 10^{12.6\pm0.3}$ Hz and a diffusion barrier of $E_d = (87 \pm 3)$ meV. We caution that the error bars result from the numerical fits of the EFM model to the data within their error margins only. Systematic errors as intrinsic in the EFM model itself and in the material constants used, as skin depth, electron-phonon coupling, electron heat capacity, and thermal conductivity that we extracted from literature (for details, see EPAPS[14]), are not included.

Nonadiabatic activation energies were determined to be about 30% larger than thermal ones [2,27] because of the reduction of multidimensional dynamics to a single reaction coordinate and because of the electronically excited state, which allows other diffusion paths than the one of lowest energy in the ground state. Consistently, the thermal diffusion energy for CO on Cu(111) is (75 ± 5) meV [28]. This difference underlines the necessity to determine nonadiabatic diffusion barriers directly.

We now turn to the process observed qualitatively in Fig. 1(b), the close approach of molecules beyond their short-range repulsion [28] that generates tilted dimers (circled). A series of STM images in Fig. 4(a) shows the step-by-step formation and decay of two tilted dimers under laser irradiation. Starting at a distance of $\sqrt{7}a$ (=fourth nearest neighboring on-top adsorption site) (I), the CO molecules jump to the $\sqrt{3}a$ distance (II) before the tilted dimer is formed (III). The dimers decay to greater distances during the next irradiation (IV).

We quantify the dimer generation rate by counting how many $\sqrt{3}$ dimers were transformed into tilted dimers by fs-laser excitation [Fig. 4(b)]. We compare this rate to the rate of arranging two noninteracting molecules on next neighboring lattice sites via fs-laser excitation, starting from a $\sqrt{3}$ configuration. For this calculation, we use the hopping rates of individual CO molecules determined above. The calculated rate for noninteracting molecules shows a decrease at higher fluences because generated dimers may decay again within a sequence of pulses.

Again, the dependence differs for photo-excited and for thermalized electrons at lower and higher fluence, respectively. For lower fluence, the calculated generation rate lies within the error bars of the calculated one, which suggests

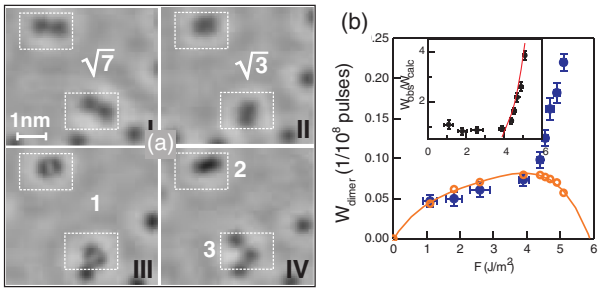

FIG. 4 (color online). Generation of tilted dimers: (a) Sequence (I–IV) of STM images resulting from fs-laser excitation with generation and decay of tilted dimers (dashed boxes), 2.5×10^8 pulses, 3.9 to 5.1 J/m^2; 35 pA, 240 mV, 7 K (b) Dependence of experimental (filled circles, from approx. 300 generated dimers; sequence of 2.5×10^8 pulses between images) and calculated (open circles) rate to generate a tilted dimer from a $\sqrt{3}$ dimer (process aII to aIII) per pulse on absorbed laser fluence; line to guide the eye; inset: Probability ratio and fit with EFM and an attraction energy of 30 meV; error bars as in Fig. 3.

that the diffusion of individual CO molecules is hardly affected by neighboring CO molecules. This result is already surprising in view of the repulsion of the molecules under thermal motion, which should reduce the number of tilted dimers. For higher fluences, the observed rate even increases strongly. This indicates a transient attraction of the usually repelling molecules.

For thermally activated processes, a difference in potential energies can be estimated from the ratio of probabilities for two different states of the system, assuming equal prefactors. Thus, the expected (R_{calc}) to the observed (R_{obs}) dimer generation rate corresponding to the state of noninteracting particles with probability P_{calc} and interacting particles with P_{obs} should satisfy: $P_{\mathrm{obs}}/P_{\mathrm{calc}} = R_{\mathrm{obs}}/R_{\mathrm{calc}} = \int e^{-\Delta E/k_B T_{\mathrm{ads}}} dt$, with ΔE the attraction energy. Neglecting the influence of photo-excited electrons on dimer generation (i.e., the fluence regime below 3.5 $\mathrm{J/m^2}$), calculated ratios are in good agreement with an attraction energy of 30 meV [Fig. 4(b), inset], which is a lower limit because of eventual thermal decay of the dimer. The tilted dimer might be a precursor state for desorption from CO saturated Cu surfaces.

Though only excited-state theory can resolve the underlying mechanism, we rationalize the enhanced dimer generation rate in a simple electrostatic picture. Therein, the excited (neutral) CO molecule diffuses toward a transiently negatively charged CO molecule. If the interacting charge distributions were represented by point charges, this process would lead to a short-range attraction of the order of several 10 meV, of the same order of magnitude as the attraction energy determined above. Such a simultaneous interaction of an excited molecule with a charged molecule is only possible under fs-laser illumination where multiple excitations (here two excitations of two neighboring molecules) are possible and as suggested by our data only at higher fluences, where the dynamics is dominated by thermalized electrons.

In conclusion, we quantitatively analyzed two nonadiabatic surface processes in real space and determined the involved activation energies: the diffusion of individual CO molecules and the generation of thermally unfavored tilted dimers. Thereby, it is revealed that both the interaction of photo-excited electrons and the one of thermalized electrons with the adsorbate degrees of freedom have to be taken into account. The formation of thermally unfavored tilted dimers demonstrates that the charge state of the adsorbate influences the diffusion path. This emphasizes the difference between adiabatic and nonadiabatic surface processes.

Our study opens an unprecedented quantitative look into the analysis of nonadiabatic surface processes at a single-molecule level and lines out future studies. Quantitative analysis of every single step of a nonadiabatic surface reaction for a broad variety of molecules, particularly in terms of site preferences, is anticipated.

We acknowledge financial support by the Deutsche Forschungsgemeinschaft.

[1] Chr. Frischkorn and M. Wolf, Chem. Rev. **106**, 4207 (2006).
[2] K. Stépán, J. Güdde, and U. Höfer, Phys. Rev. Lett. **94**, 236103 (2005).
[3] E. H. G. Backus, A. Eichler, A. W. Kleyn, and M. Bonn, Science **310**, 1790 (2005).
[4] M. Mehlhorn, H. Gawronski, and K. Morgenstern, Phys. Rev. Lett. **101**, 196101 (2008).
[5] L. Bartels, F. Wang, D. Möller, and T. F. Heinz, Science **305**, 648 (2004).
[6] M. Mehlhorn, H. Gawronski, L. Nedelmann, A. Grujic, and K. Morgenstern, Rev. Sci. Instrum. **78**, 033905 (2007).
[7] More precisely, the pulses are divided into 125 trenches of 0.2 s length, and the trenches are separated by 10 s in order to minimize effects due to heat accumulation.
[8] R. Raval *et al.*, Surf. Sci. **203**, 353 (1988).
[9] A. J. Heinrich, C. P. Lutz, J. A. Gupta, and D. M. Eigler, Science **298**, 1381 (2002).
[10] E. Niemi and J. Nieminen, Chem. Phys. Lett. **397**, 200 (2004).
[11] M. Persson, Phil. Trans. R. Soc. A **362**, 1173 (2004).
[12] Sven Zoephel, Ph.D. thesis, FU Berlin, 2000.
[13] G. Ehrlich, J. Chem. Phys. **44**, 1050 (1966).
[14] See supplementary materials at http://link.aps.org/supplemental/10.1103/PhysRevLett.104.076101 for an extraction of hopping rates per pulse from hopping distributions and for details on the electronic friction model used.
[15] J. Repp, F. Moresco, G. Meyer, K. H. Rieder, P. Hyldgaard, and M. Persson, Phys. Rev. Lett. **85**, 2981 (2000).
[16] S. Deliwala, R. J. Finlay, J. R. Goldman, T. H. Her, W. D. Mieher, and E. Mazur, Chem. Phys. Lett. **242**, 617 (1995).
[17] D. G. Busch, W. Ho, Phys. Rev. Lett. **77**, 1338 (1996).
[18] M. Lisowski, P. A. Loukakos, U. Bovensiepen, J. Stähler, C. Gahl, and M. Wolf, Appl. Phys. A **78**, 165 (2004).
[19] L. Bartels *et al.*, Phys. Rev. Lett. **80**, 2004 (1998).
[20] M. Wolf, A. Hotzel, E. Knoesel, and D. Velic, Phys. Rev. B **59**, 5926 (1999).
[21] T. Komeda, Y. Kim, M. Kawai, B. N. J. Persson, and H. Ueba, Science **295**, 2055 (2002).
[22] J. I. Pascual, N. Lorente, Z. Song, H. Conrad, and H.-P. Rust, Nature (London) **423**, 525 (2003).
[23] S. I. Anisimov, P. L. Kapeliovich, and T. L. Perel'man, Sov. Phys. JETP **66**, 776 (1974).
[24] S. I. Anisimov and B. Rethfeld, Proc. SPIE Int. Soc. Opt. Eng. **3093**, 192 (1997).
[25] F. Budde, T. F. Heinz, A. Kalamarides, M. M. T. Loy, and J. A. Misewich, Surf. Sci. **283**, 143 (1993).
[26] L. M. Struck, L. J. Richter, S. A. Buntin, R. R. Cavanagh, and J. C. Stephenson, Phys. Rev. Lett. **77**, 4576 (1996).
[27] A. C. Luntz, M. Persson, S. Wagner, C. Frischkorn, and M. Wolf, J. Chem. Phys. **124**, 244702 (2006).
[28] K. L. Wong, B. V. Rao, G. Pawin, E. Ulin-Avila, and L. Bartels, J. Chem. Phys. **123**, 201102 (2005).
[29] L. Bartels, G. Meyer, and K. H. Rieder, Appl. Phys. Lett. **71**, 213 (1997).